Materials Research Proceedings 41 (2024) 871-880 https://doi.org/10.21741/9781644903131-95

Surrogate model to describe temperature field in real-time for hot forging

MIDAOUI Aya[1,a *], BAUDOUIN Cyrille[1,b], DANGLADE Florence[2,c] and BIGOT Régis[1,d]

[1]HESAM Université, Arts et Métiers Institute of Technology, Université de Lorraine, LCFC, 57070 Metz, France

[2] HESAM Université, Arts et Métiers Institute of Technology, LISPEN, F-71100 Chalon-sur-Saône, France

[a]aya.midaoui@ensam.eu, [b]cyrille.baudouin@ensam.eu, [c]florence.danglade@ensam.eu, [d]regis.bigot@ensam.eu

Keywords: Hot Forging, Proper Orthogonal Decomposition, Numerical Simulations, Surrogate Model, Real-Time Monitoring System

Abstract. In the context of certain metallic alloys, the conformity of the product depends on its metallurgical structure. Addressing this, the implementation of a real-time monitoring system to control the evolution of the metallurgical structure and the geometry of the cogging part is proposed. Focusing on the microstructure's dependence on temperature, this article outlines the requested steps for developing data-driven reduced models for describing the temperature field in the billet. These models use temperature data collected from predictive numerical simulations conducted using FORGE® software. Applying the Proper Orthogonal Decomposition (POD) technique, the images illustrating the temperature field are reconstructed through a 2D matrix-based framework. This matrix, derived from non-discretized elements issued from FORGE®, underwent discretization through an objective method, resulting in a size of 100*100. The utilization of the POD technique in this approach provides a parametric vector description, facilitating rapid image reconstruction through manipulation of vector system parameters. With just two vectors, we can effectively reconstruct the image representing the temperature field.

Introduction

Forging at high temperatures plays a crucial role in metallurgy, as hot deformation influences the microstructure of the product, which dictates product conformity and performance. The microstructure depends on several factors: temperature, deformation, deformation rate, and their temporal evolution [1], [2]. In this context, our focus is primarily on temperature.

Hot forming processes induce strong temperature gradients with rapid fluctuations over time. These variations arise from thermal exchanges with the tool, interaction with air at exposed surfaces, and adiabatic heating resulting from plastic deformation [3]. Each forging sequence involves a transfer time from the furnace to the press, a waiting time on the tooling, a shaping operation, and finally a cooling time. These fluctuations lead to both metallurgical and geometrical deviations from the intended target [4].

In the case of a manual cogging operation, our goal is to provide the operator with a temperature field mapping in real time to assist in decision-making. This system, using sensors and prediction models, will reconstruct in real-time the temperature field within a section (2D image plane) of the billet through extrapolation. Consequently, it will assist in adapting process control parameters during the operation.

While existing simulation models can predict temperature [5], the calculation time depends on the desired result accuracy, posing challenges when reactivity is essential [6]. This is especially

pertinent in the case of hot forging, characterized by significant temperature shifts. Any delay in generating the temperature field image could result in the loss of crucial information for effective process control. So, surrogate models are employed to replace Finite Element Method (FEM) resolution by a simplified alternative description, that link essential connections between input variables and output responses. They are usually used for real time predictions, sticking an equilibrium between reactivity and accuracy [7], [8].

Some applications require surrogate models to describe fields, such as temperature field within air-conditioned spaces [9]. Proper Orthogonal Decomposition is used to construct such models by reducing their dimensionality, resulting in POD-based surrogate models[10], [11]. The Proper Orthogonal Decomposition (POD) is applied for image compression through a vectoral description. Sorting the vectors in the description basis by importance allows for a reduction in computational time, as only the dominant vectors are retained, effectively reducing the dimensionality of the basis. Although there has been extensive research on surrogate models in predicting temperature fields in architectural and energy contexts [12], [13], their applicability in forecasting temperature fields in metal forming processes has not been thoroughly investigated.

Hence, the focal point on this research lies in predicting temperature fields within metal processes. This work involves collecting temperature data from FORGE® Finite Element simulations as the initial step [14]. FORGE® is a numerical simulation software for forging (or shaping) operations, distinguished by its adaptive remeshing during simulations. To apply the Proper Orthogonal Decomposition (POD) technique, the mesh must maintain a constant number of points, and it is imperative to know the position of these points when reconstructing an image. Therefore, we propose a technique that transforms FORGE's unordered automatic mesh into a matrix-like structure representing the pixels of an image. Subsequently, the POD technique will be applied to determine a vector basis capable of describing the image, selecting the number of dominant vectors to optimize computation time. The image can then be reconstructed from this vector basis. In this paper, we will focus on the initial phases where the billet is not yet deformed. However, our goal is to generalize the techniques so that they are applicable to any section, even when deformation occurs. The aim of this research is to objectively determine the size of the matrix structure and subsequently the number of vectors required to reconstruct an image. The initial effort focused on establishing a tool capable of swiftly calculating this image at each time step, minimizing deviations from the numerical simulation, by setting criteria such as a temperature mean difference below 1°C and a gradient with pixel differences under 5 °C.

Materials

Numerical simulations were performed using the commercial FORGE® software developed by Transvalor. As a first step, the focus is on monitoring the temperature field during the transfer of a billet, specifically made of XC35 steel with a diameter of 45 mm and a height of 65 mm, from the furnace to the press.

We suppose that the billet stays at least 30 minutes in the furnace, so it is assumed to have a homogeneous temperature of 1200 °C. Transported to the press using a gripper, the transfer time of the billet is estimated at a maximum of 8 s. FORGE® allows the adjustment of those various parameters, including the thickness of the gripper (20 mm) and the length of the contact surface (37 mm) between the gripper and the billet.

The contact between the gripper and the billet is considered partial, with specific pressure applied to prevent the piece from falling. In fact, the chosen heat transfer coefficient is estimated at 3000 W/m^2K[14], and at 10 W/m^2K between the air and the billet. The thermal conductivity of the material is 35.5 W/m^2K. The room temperature is 25 °C, which is also the initial temperature of the gripper. Friction conditions follow a Coulomb limited Tresca Model (Eq. 1):

$$\tau = \min(\mu \cdot \sigma_n ; m \cdot \frac{\sigma_0}{\sqrt{3}}). \quad (1)$$

where σ_n is the contact pressure; μ and m the friction coefficients, equal to 0.4 and 0.8, respectively.

Using finite element methods, the billet mesh is composed to tetrahedrons with a maximum mesh size of 1.14 mm and provides temperatures corresponding to each coordinate point (Xi, Yi, Zi) belonging to the mesh nodes (11190). These data are crucial for image reconstruction as they represent input parameters.

Time increments are defined at 0.5 s, resulting in 16-time steps ranging from 0.5 s to 8 s. Since each temperature field corresponds to a specific time, 16 images will represent the temperature fields.

Methods

The methodology involves extracting temperature data from FORGE® simulation (Fig. 1a). Interpolations transform FORGE's mesh into ordered matrix image representing temperature field (Fig. 1b). Subsequently, the Proper Orthogonal Decomposition (POD) technique is applied to optimize computation time by selecting dominant vectors for image description (Fig. 1c)

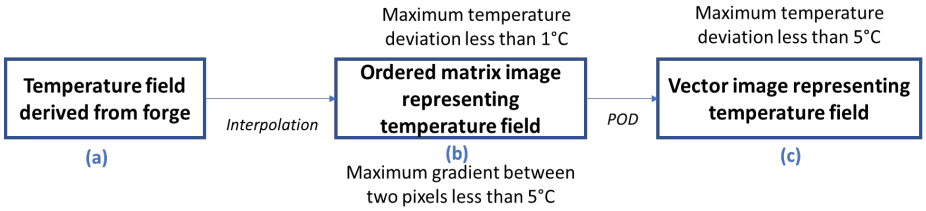

Fig.1. Methodology.

Ordered discretization (b). Given the irregular mesh in FORGE®, where the number of elements in the simulation's mesh depends on the billet's size, coupled with FORGE® regularly performing remeshing during simulations, it is uncommon to have a constant number of points and to track the evolution of the same point. Therefore, the decision was made to describe the temperature field of a section using a regular grid (Matrix image with pixels arranged in rows and columns.). For each calculation increment, the grid should represent the temperature field. To achieve this, various interpolation techniques were employed to recalculate the temperature at grid points that do not correspond to the coordinates of nodes extracted from the numerical simulation in FORGE®. The employed interpolation methods include Inverse Distance Weighting [15], nearest neighbor interpolation [16], 2D linear interpolation using Delaunay triangulation [17], cubic spline interpolation [18], and local polynomial interpolation.

The choice of the interpolation method relies on the examination of the error between numerical simulation temperature values and those interpolated at the same coordinates, as well as the Pearson correlation coefficient that measures the linear correlation between two sets of data.

The next step is to objectively determine the size of the structured grid (rectangular) needed to describe the temperature field. To achieve this objective, an analysis is undertaken to establish objective criteria that will define the number of points required on this grid.

Across various grids of different sizes, memory space, computation time, the average of differences of the mean temperatures (Eq. 2), and the maximum of differences of the mean temperatures (Eq. 3) for the 16-time steps (corresponding to the 16 images representing the temperature field) between interpolated temperature values corresponding to changes in grid size $\hat{T}_{grid}$ ranging from 10x10 to 100 x100 and the numerical simulation tool temperature $\hat{T}_{fem}$ values were calculated.

$$\frac{\sum_{k=1}^{16}\left|\hat{T}_{fem_k} - \hat{T}_{grid_k}\right|}{16} \quad (2)$$

$$max_{k=1}^{16}\left(\left|\hat{T}_{fem_k} - \hat{T}_{grid_k}\right|\right) \quad (3)$$

A study has also been conducted on the visual aspect of the reconstructed image. To assess the quality of the reconstructed image, the criterion considered is the study of image sharpness. To quantify this quality, the Sobel operator is employed [19], which serves to measure the sharpness of the image by calculating the intensity gradients (Eq. 5) of the image with respect to its horizontal (Eq. 4.1) and vertical (Eq. 4.2) coordinates.

$$G_x = \begin{bmatrix} -1 & 0 & 1 \\ -2 & 0 & 2 \\ -1 & 0 & 1 \end{bmatrix} * A \qquad G_y = \begin{bmatrix} -1 & -2 & -1 \\ 0 & 0 & 0 \\ 1 & 2 & 1 \end{bmatrix} * A \quad (4.1\ 4.2)$$

$$G=\sqrt{gradient(x)^2 + gradient(y)^2} \quad (5)$$

The mean gradient magnitude curve is computed for each grid image, spanning dimensions from 10x10 to 100x100.This curve provides an assessment of the image's overall sharpness. A heightened gradient magnitude signals abrupt intensity changes between pixels, indicating significant variations in the image. Conversely, a lower magnitude denotes a smoother image, where transitions between pixel grayscale levels are more gradual.

In this context, a low gradient magnitude is of particular importance, as it indicates subtle intensity variations between pixels. This is relevant in our case because the observed temperature changes are minimal. Therefore, an image displaying a low gradient intensity is more pertinent for our analytical objective.

Proper Orthogonal Decomposition (c). At this point, we have successfully reconstructed each image (for every increment) in a pixelated format. Our current objective is to represent the entire set of these images using a unified vector basis. To achieve this, we leverage the image collection and apply the POD technique. As a vector-based method, POD enables us to derive a vector basis, allowing us to describe each image through a linear combination of these vectors. Consequently, this approach ensures a brief computational time in the end. This technique, originating from image processing (as a temperature field can be viewed as an image), involves describing a mesh with a constant number of nodes through a linear combination of eigenvectors. The Proper Orthogonal Decomposition technique serves this propose, enabling the characterization of fields through a parameterized vector system that captures their predominant features or patterns[20]. By deliberately selecting the most influential vectors, often referred to as modes, this technique effectively reduces the volume of data required for precise representation of temperature fields.

After reconstructing the 16 grids, they are assembled into a matrix where each column represents all the points at a given increment, and each row depicts the temperature evolution at each point over the course of the 16 increments.

Using Proper Orthogonal Decomposition (POD), the most influential vectors are extracted, commonly known as eigenvectors. These eigenvectors are sorted in descending order based on their corresponding eigenvalues. The model reduction technique involves retaining only a reduced yet significant number of eigenvectors to accelerate the computation and refreshing of the image. Subsequently, images could be generated with reconstructions using varying numbers of modes : 1 mode, 2 modes, 5 modes, etc. The initial task is to identify the minimum number of modes necessary to achieve the reconstruction of the temperature matrix with the deviation less than 5

°C. This evaluation involves comparing each reconstructed image from different modes with the selected regular grid image.

At the end of this section, pivotal questions emerge, steering the trajectory of our investigation. Firstly, what interpolation technique best ensures the precision of our data representation? Secondly, what grid size strikes the optimal balance, achieving a maximum temperature difference of 1 °C and an average maximum gradient of 5 °C? Finally, how many proper vectors are required for a lossless image reconstruction, with a maximum temperature difference of 5 °C? These questions serve as crucial benchmarks, guiding our pursuit of effective methodologies and contributing to the broader applicability of our techniques, even in scenarios involving deformation.

Results

Optimal Interpolation Technique. After a thorough evaluation of the various interpolation methods (Fig. 2) discussed in the previous paragraph, it is concluded 2D linear interpolation based on Delaunay triangulation emerges as the optimal approach for temperature prediction in this case. This conclusion is drawn as it consistently demonstrated the smallest average deviation (0.12 for the average of deviations across all 16-time steps) and the Pearson coefficient closest to 1 (0.9990 for the average of Pearson coefficients for all time steps). It's worth noting that a Pearson coefficient of 1 indicates a perfect linear correlation.

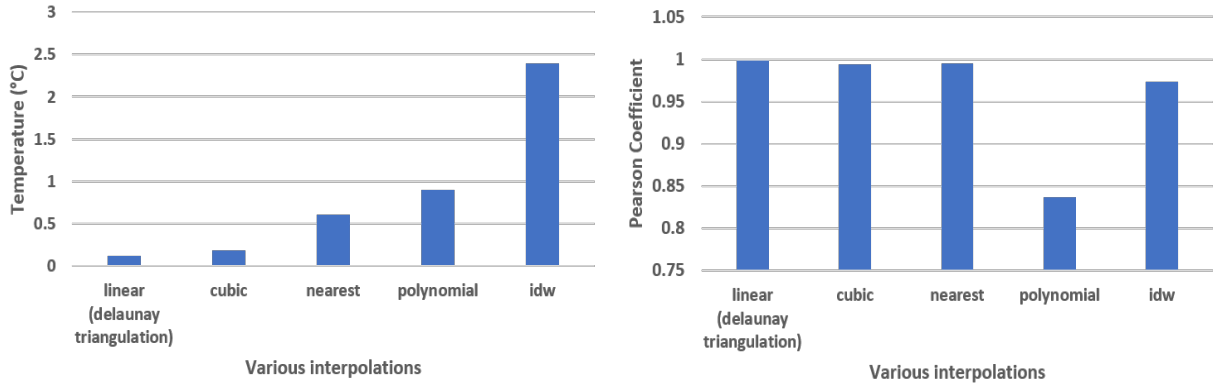

Fig. 2. Comparative study of average deviation of temperature (°C) and Pearson coefficient for various interpolations

Grid Size for Max Temperature Difference of 1 °C and Average Gradient of 5 °C. Analyzing the computation time for grids ranging from 10x10 to 100x100 reveals minimal change, hovering between 0.111 s and 0.116 s. Similarly, when examining memory space, the variance is not substantial, fluctuating between 164.7 Mo and 166 Mo. Since these metrics show negligible differences, our focus shifts to evaluating the other criteria mentioned earlier to determine the dimension of the structured (rectangular) grid needed to describe the temperature field with a deviation of less than 1 °C compared to the numerical simulation, the result is that a grid of at least (100*100) points is required to meet the criteria (Fig. 3).

A study was also conducted on the visual quality of the reconstructed image to ensure it is not overly "pixelated". According to the equation (Eq. 5), the vertical and horizontal gradients (Fig. 4) for two grid (50*50) and (100*100) are obtained below. The appearance of the image is influenced by cold spots generated by the clamps.

In our case, the objective is to generate an image where the temperature variation between 2 pixels should be less than 5 °C.

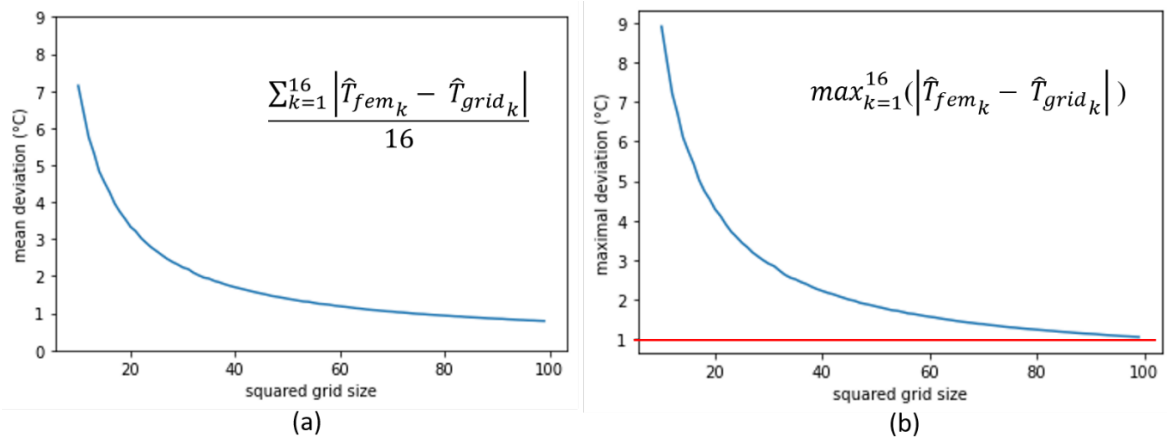

Fig. 3. Evaluation of mean (a) and maximal (b) deviations from the average temperature depending on grid size.

The analysis of the gradient magnitude reveals that when there is a temperature variation of less than 5 °C between two pixels, it is advisable to use a grid size of at least 100x100 (Fig. 4). The combination of all criteria leads to a choice of 100*100.

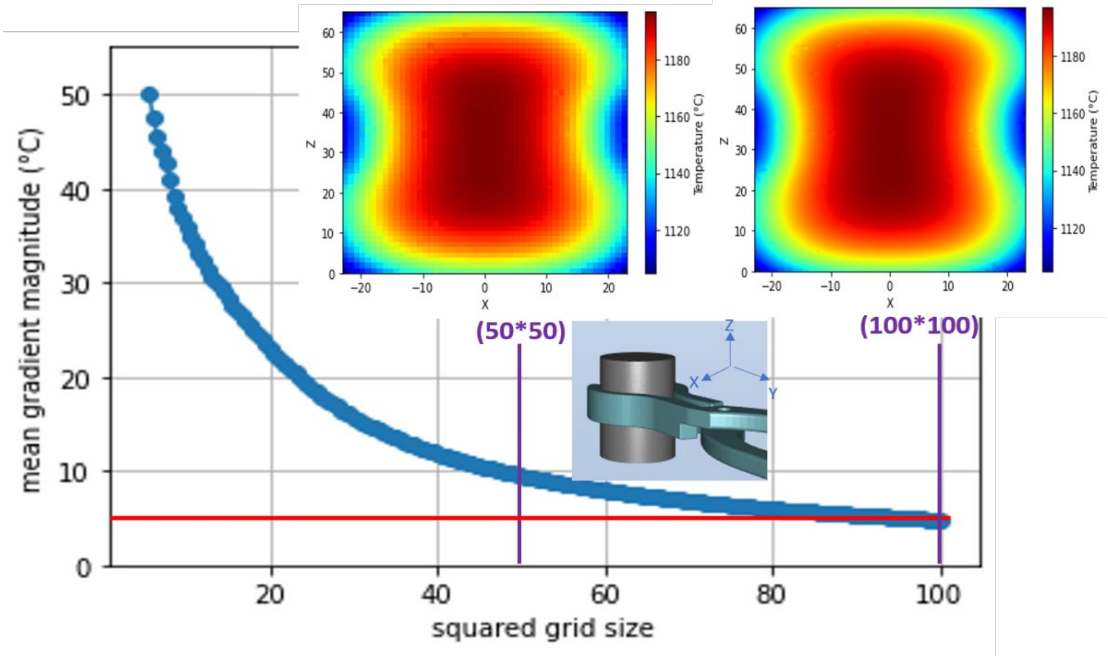

Fig. 4. Curve of the mean gradient magntiude and images pixelized of temperature field for 2 grid sizes.

Number of eigenvectors for Lossless Image Reconstruction. In this section, the approach involves reconstructing an image with a vectorized description using different numbers of eigenvectors ranging from 1 to 16. The process includes taking the collection of 16 images and generating a reconstructed image for each case. The evaluation focuses on examining the maximum error at a specific point between the reconstructed image and the pixelated image (100*100) (Fig. 5). Subsequently, the maximum error across all time increments (16) is determined.

To achieve a maximum error of 5 °C, the addition of eigenvectors is deemed necessary; however, this comes at the expense of increased computation time. Opting for a compromise, a reduction of 6 °C is accepted, resulting in a conservation of vectors and a corresponding reduction

in computational expenses. Considering the ambient temperature is 1200 °C and the current error stands at 6 °C, this signifies a deviation margin of approximately 0.5%. Consequently, the decision has been made to adhere to 2 eigenvectors striking a balance between precision and computational load. Nonetheless, in cases where specific requirements demand heightened accuracy, the option to include more modes remains available. While this approach doesn't inherently introduce greater technical complexity, it does entail a trade-off with increased computation time.

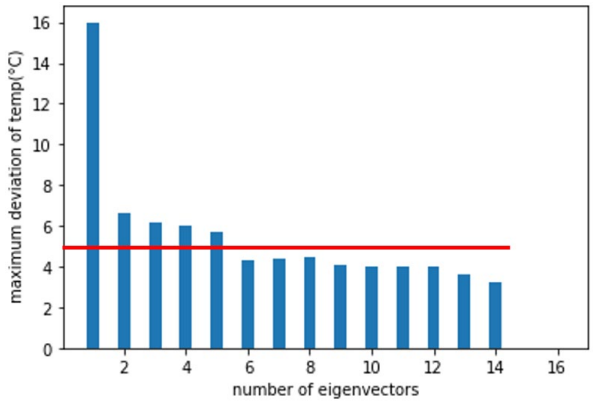

Fig.5. Maximal deviation of temperature based on the number of eigenvectors.

With these 2 eigenvectors, and by interpolation, the temperature image can be reconstructed at any given time. The ensuing figure (Fig. 6) illustrate the coefficients of these 2 eigenvectors over time.

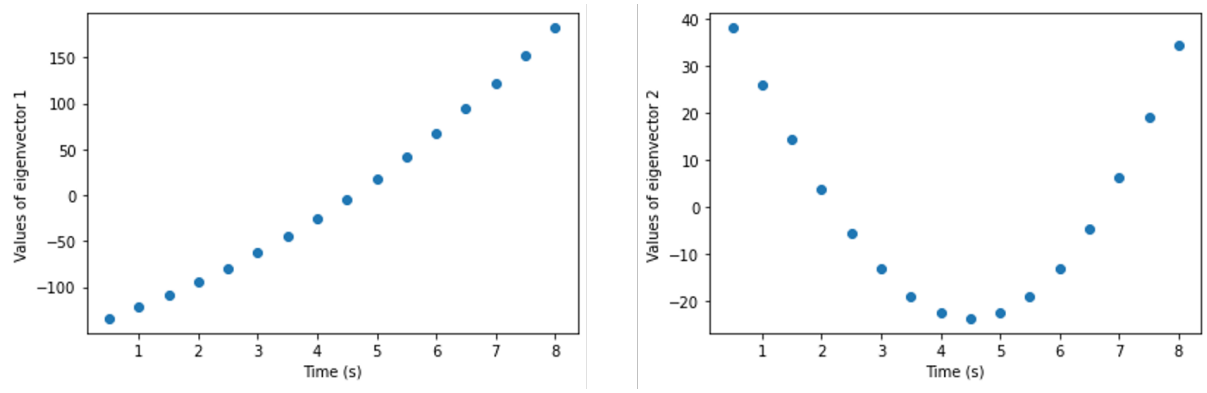

Fig. 6. Eigenvectors values resulting from POD.

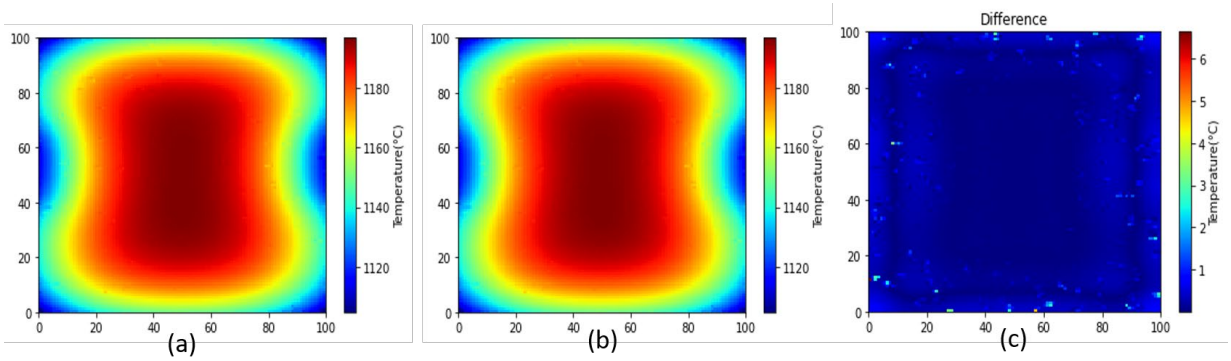

Fig. 7. Temperature field represented by ordered matrix image(a), and by vector image(b), and the difference(c).

The figure 7 depicts the temperature field represented by ordered matrix image (Fig. 7a), and by vector image (Fig. 7b), as well as the difference between the two (Fig. 7c). It appears that there

are some numerical errors that warrant a more detailed analysis of the interpolation algorithms. Despite the field exhibiting a constant evolution, there are occasional discrepancies that do not follow a consistent trend. Further scrutiny of the interpolation algorithms is necessary to address these discrepancies and ensure a more accurate representation of the temperature field.

Discussion

To represent temperature fields, several considerations arise:

- Interpolation Method: The process of discretizing and standardizing temperature fields involves inherent errors, making the careful selection of an appropriate interpolation method crucial to minimize these inaccuracies. In our study, we chose a method based on Delaunay triangulation to perform the interpolation. While this approach addresses many concerns, it is essential to acknowledge the potential edge effects that may arise. It is important to note that the technique remains applicable in a three-dimensional (3D) context, offering versatility in addressing temperature variations throughout the spatial domain.
- The Grid Size Selection: The selection of an appropriate grid size is a crucial factor, influencing our ability to accurately capture the entire temperature field akin to the finite element simulation. In our investigation, a grid size of 100x100 stands out as the most fitting choice. This particular grid size ensures a sufficient number of elements to closely replicate the nuances of the finite element simulation's temperature distribution. However, it's worth noting that the grid size can be easily adapted by modifying the criteria. It would be judicious to consider the sensor sensitivity when adjusting the grid size to align with the measurements we will be able to obtain
- Number of Modes (eigenvectors): Careful thought needs to be given to choosing the number of modes, considering their sensitivity to variations in the temperature field. While vector addition is computationally efficient, it is crucial to note that we are not restricted to a specific number of modes. However, it's essential to acknowledge that recalculating an image quickly is feasible. Still, due to various assumptions made, such as thermal exchanges, we cannot solely rely on post-furnace time for image recalculation. Additionally, having temperature measurements is necessary to recalibrate the coefficients of the vector combination at measurement points, enabling the propagation of the image across the entire section.

Since Proper Orthogonal Decomposition (POD) enables the faithful reconstruction of an image of temperature field consistent with finite element simulations, we propose to extend this methodology to subsequent phases with the same interpolation method, and grid size. This includes the positioning of the billet onto the press and its subsequent shaping.

The scientific challenge at this stage lies in chaining reduced models without necessarily having to redo the numerical experimental plan from the beginning of the process. We also plan to extend our modeling to a three-dimensional representation of the temperature field. Additionally, the introduction of a deformable mesh will need to be considered, particularly when working on cogging operations.

Next, the alignment of reduced models with reality, involving the adjustment of linear combination parameters based on temperature measurement data, poses an additional scientific challenge. Simultaneously, we are exploring two distinct paths to address this challenge:

a) Continuation of the Process: Despite the scientific challenges, our focus remains on advancing the process to generate an image at various stages, irrespective of the phase of the manufacturing process. This involves refining the models and incorporating real-time temperature data, ensuring a comprehensive representation.

b) Demonstrator Development: In parallel, we are working towards the development of a demonstrator that integrates sensors for real-time data collection and visualization. However, we recognize the importance of adapting the form of feedback for optimal operator interpretation. Traditional image returns might not be the most straightforward. Therefore, alternative presentation forms, often referred to as metaphors, are being explored.

Ultimately, our long-term goal is to create additional metamodels predicting various fields impacting the microstructure. Real-time presentation of grain sizes and deformations directly to the blacksmith could offer substantial benefits. The success of these solutions will be validated through the creation of a demonstrator once all the necessary tools are operational. This approach allows us to materialize our vision of integrating augmented reality to assist operators in decision-making.

Conclusion

This paper deals with a methodology to obtain a picture representing a temperature field of a billet section in real-time during a forging process. Our research illustrates the capability of describing an image using a vector system, effectively reduced through the application of Proper Orthogonal Decomposition (POD) techniques. However, achieving this necessitates an image with a consistent and known number of points in space. We have established a methodology to reconstruct a 2D matrix image from a non-uniformly distributed Finite Element Method (FEM) mesh. This methodology enables the objective determination of tool parameters, including grid size and the number of vectors employed, ensuring a standardized and principled approach to image reconstruction.

Acknowledgments

I extend my sincere thanks to CETIM (Centre Technique des Industries Mécaniques) and the Region Grand Est for their financial support in funding this thesis. Their contribution has been instrumental in the successful completion of my research.

References

[1] H. Clemens, S. Mayer, et C. Scheu, « Microstructure and Properties of Engineering Materials », in Neutrons and Synchrotron Radiation in Engineering Materials Science, John Wiley & Sons, Ltd, 2017, p. 1-20.

[2] G. Y. Lai, W. E. Wood, R. A. Clark, V. F. Zackay, et E. R. Parker, « The effect of austenitizing temperature on the microstructure and mechanical properties of as-quenched 4340 steel », Metall Trans, vol. 5, no 7, p. 1663-1670, juill. 1974. https://doi.org/ 10.1007/BF02646340

[3] R. Douglas et D. Kuhlmann, « Guidelines for precision hot forging with applications », Journal of Materials Processing Technology, vol. 98, no 2, p. 182-188, janv. 2000. https://doi.org/ 10.1016/S0924-0136(99)00197-1

[4] Z. Allam, E. Becker, C. Baudouin, R. Bigot, et P. Krumpipe, « Forging Process Control: Influence of Key Parameters Variation on Product Specifications Deviations », Procedia Engineering, vol. 81, p. 2524-2529, janv. 2014. https://doi.org/ 10.1016/j.proeng.2014.10.361

[5] Y. C. Gerstenmaier et G. Wachutka, « Time dependent temperature ®elds calculated using eigenfunctions and eigenvalues of the heat conduction equation », Microelectronics Journal, 2001.

[6] J. Yin, R. Hu, et X. Shu, « Closed-die forging process of copper alloy valve body: finite element simulation and experiments », Journal of Materials Research and Technology, vol. 10, p. 1339-1347, janv. 2021. https://doi.org/ 10.1016/j.jmrt.2020.12.087

[7] P. Ruane, P. Walsh, et J. Cosgrove, « Development of a digital model and metamodel to improve the performance of an automated manufacturing line », Journal of Manufacturing Systems, vol. 65, p. 538-549, oct. 2022. https://doi.org/ 10.1016/j.jmsy.2022.10.011

[8] L. Jia, R. Alizadeh, J. Hao, G. Wang, J. K. Allen, et F. Mistree, « A rule-based method for automated surrogate model selection », Advanced Engineering Informatics, vol. 45, p. 101123, août 2020. https://doi.org/ 10.1016/j.aei.2020.101123

[9] B. Jiang, H. Gong, H. Qin, et M. Zhu, « Attention-LSTM architecture combined with Bayesian hyperparameter optimization for indoor temperature prediction », Building and Environment, vol. 224, p. 109536, oct. 2022. https://doi.org/ 10.1016/j.buildenv.2022.109536

[10] B. M. de Gooijer, J. Havinga, H. J. M. Geijselaers, et A. H. van den Boogaard, « Evaluation of POD based surrogate models of fields resulting from nonlinear FEM simulations », Advanced Modeling and Simulation in Engineering Sciences, vol. 8, no 1, p. 25, nov. 2021. https://doi.org/ 10.1186/s40323-021-00210-8

[11] D. Uribe, C. Baudouin, C. Durand, et R. Bigot, « Predictive control for a single-blow cold upsetting using surrogate modeling for a digital twin », Int J Mater Form, vol. 17, no 1, p. 7, déc. 2023. https://doi.org/ 10.1007/s12289-023-01803-x

[12] W. Yoo, M. J. Clayton, et W. Yan, « ESMUST: EnergyPlus-driven surrogate model for urban surface temperature prediction », Building and Environment, vol. 229, p. 109935, févr. 2023. https://doi.org/ 10.1016/j.buildenv.2022.109935

[13] Y. Liu, G. Lin, J. Guo, et J. Zhu, « Dynamic prediction of fuel temperature in aircraft fuel tanks based on surrogate », Applied Thermal Engineering, vol. 215, p. 118926, oct. 2022. https://doi.org/ 10.1016/j.applthermaleng.2022.118926

[14] T. S.A, « Ressources | FORGE® ». https://www.transvalor.com/fr/ressources/tag/forge (consulté le août 22, 2023).

[15] A. Saha, B. S. Gupta, S. Patidar, et N. Martínez-Villegas, « Spatial distribution based on optimal interpolation techniques and assessment of contamination risk for toxic metals in the surface soil », Journal of South American Earth Sciences, vol. 115, p. 103763, avr. 2022. https://doi.org/ 10.1016/j.jsames.2022.103763

[16] R. M. Di Biase, A. Marcelli, S. Franceschi, A. Bartolini, et L. Fattorini, « Design-based mapping of plant species presence, association, and richness by nearest-neighbour interpolation », Spatial Statistics, vol. 51, p. 100660, oct. 2022. https://doi.org/ 10.1016/j.spasta.2022.100660

[17] Y. Liu et G. Yin, « The Delaunay triangulation learner and its ensembles », Computational Statistics & Data Analysis, vol. 152, p. 107030, déc. 2020. https://doi.org/ 10.1016/j.csda.2020.107030

[18] M. Sun, L. Lan, C.-G. Zhu, et F. Lei, « Cubic spline interpolation with optimal end conditions », Journal of Computational and Applied Mathematics, vol. 425, p. 115039, juin 2023. https://doi.org/ 10.1016/j.cam.2022.115039

[19] O. Vincent et O. Folorunso, « A Descriptive Algorithm for Sobel Image Edge Detection », présenté à InSITE 2009: Informing Science + IT Education Conference, 2009. https://doi.org/ 10.28945/3351.

[20] S. L. Brunton et J. N. Kutz, « Data Driven Science & Engineering », 2017.